PHILOSOPHICAL TRANSACTIONS OF THE ROYAL SOCIETY A

Phil. Trans. R. Soc. A (2005) **363**, 2811–2835
doi:10.1098/rsta.2005.1675
Published online 31 October 2005

The physical and chemical composition of the lower mantle

By C. Isabella Bovolo*

School of Civil Engineering & Geosciences, University of Newcastle upon Tyne,
Newcastle upon Tyne NE1 7RU, UK
(isabella.bovolo@ncl.ac.uk)

This article reviews some of the recent advances made within the field of mineral physics. In order to link the observed seismic and density structures of the lower mantle with a particular mineral composition, knowledge of the thermodynamic properties of the candidate materials is required. Determining which compositional model best matches the observed data is difficult because of the wide variety of possible mineral structures and compositions. State-of-the-art experimental and analytical techniques have pushed forward our knowledge of mineral physics, yet certain properties, such as the elastic properties of lower mantle minerals at high pressures and temperatures, are difficult to determine experimentally and remain elusive. Fortunately, computational techniques are now sufficiently advanced to enable the prediction of these properties in a self-consistent manner, but more results are required.

A fundamental question is whether or not the upper and lower mantles are mixing. Traditional models that involve chemically separate upper and lower mantles cannot yet be ruled out despite recent conflicting seismological evidence showing that subducting slabs penetrate deep into the lower mantle and that chemically distinct layers are, therefore, unlikely.

Recent seismic tomography studies giving three-dimensional models of the seismic wave velocities in the Earth also base their interpretations on the thermodynamic properties of minerals. These studies reveal heterogeneous velocity and density anomalies in the lower mantle, which are difficult to reconcile with mineral physics data.

Keywords: lower mantle composition; mineral physics; elastic constants

1. Introduction

Why do the magnetic poles of the Earth reverse? What drives the geodynamo? What is the Earth made of? Such fundamental questions regarding the Earth remain unresolved. This paper attempts to review the state-of-the-art and some of the debate surrounding just one issue—the mantle's composition, particularly the lower mantle's composition. Although the mantle and core are almost equal in thickness, the mantle occupies 84% of the Earth by volume, whereas the core

---

*Work carried out at Department of Earth Sciences, University of Bristol, Bristol BS8 1RJ, UK.

One contribution of 17 to a Triennial Issue 'Astronomy and earth science'.

© 2005 The Royal Society

occupies only 15%. The lower mantle is the largest continuous region in the Earth, occupying 55% of the Earth by volume (Dziewonski & Anderson 1981). Its chemical composition (what it is made of) and its constituent mineralogy (its structure) are not known sufficiently accurately to dispel arguments over mantle mixing and the origin and causes of seismic anisotropy (the change in seismic property with change of direction). Recent work, however, pushes our knowledge forward and gives us new insight into these intricate subjects.

This paper is structured as follows: I start by giving an overview of the lower mantle in a planetary context and then describe the problem in terms of mineral physics. There are several experimental and computational improvements that have been made recently and I give a broad overview of these. These techniques help us to define the thermodynamic and elastic properties of lower mantle minerals, which are needed to interpret the observed lower mantle properties in terms of its chemical and physical composition. I describe the basic structures of the three main lower mantle minerals and review the most up-to-date results. Unfortunately, these data do not give us the whole story. Complications arise owing to compositional variations within the minerals. Iron (both ferric, Fe^{3+}, and ferrous, Fe^{2+}), aluminium, calcium and water are present in the lower mantles and their presence is known to alter the properties of the basic mantle minerals. I briefly describe our current knowledge of some of these effects and also describe the partitioning of iron between the minerals.

The uncertainties associated with the properties of the lower mantle minerals lead to several possible lower mantle compositional models, each having different and significant implications for the evolution of the Earth. Some of these different models are introduced and their implications discussed in terms of lower mantle mixing and the nature of the boundary between the upper and lower mantles. Recent seismic tomography studies have revealed seismic anomalies in the lower mantle through unexpected correlations and anti-correlations between compressional- and shear-wave velocities. Several explanations for these phenomena have been put forward and are reviewed. All of these interpretations, however, rely on mineral physics data. These data, as we shall see, are the key to correctly interpreting the state of the lower mantle and the evolution of the Earth. Unfortunately, getting hold of this data is not easy…

2. The lower mantle in a planetary context

The Earth has a radius of 6371 km, yet the deepest boreholes reach to a depth of only 12 km. As we cannot probe the inner Earth directly, our knowledge of its interior stems mainly from indirect evidence. Studies of the chemistry of the Solar System and the composition of meteorites can give us broad bounds on the chemistry of the Earth as a whole. Geochemical evidence from magma and rock fragments brought tectonically to the surface from depths of 200 km together with geophysical evidence such as density and magnetic studies and, in particular, seismic studies allow us to constrain further the Earth's composition and structure.

It is now generally accepted that the Earth's interior consists of several almost concentric spheres. The outer, thin and brittle crust averages 7 km beneath the

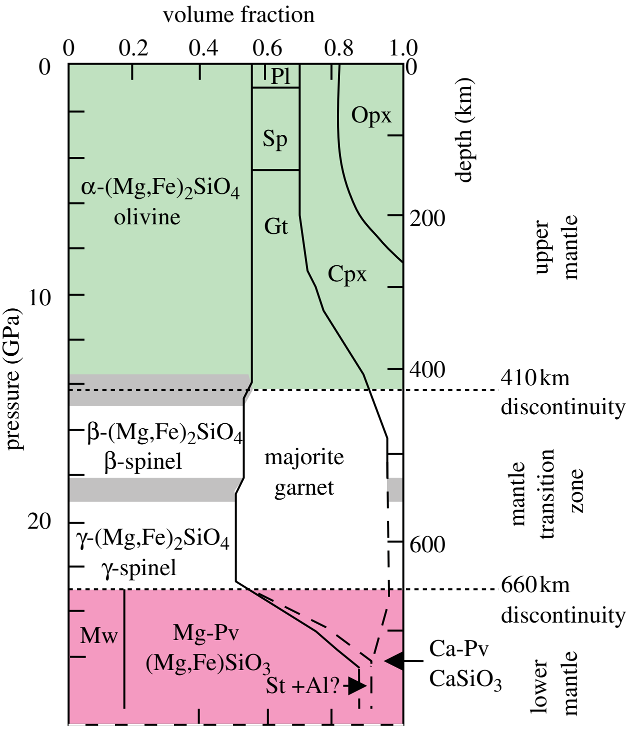

Figure 1. Schematic of the volumetric mineral constitution of a peridotite mantle down to the lower mantle (modified after Ito & Takahashi 1987). Peridotite is a dense coarse-grained igneous rock consisting mainly of olivine and pyroxene. It is high in Fe and Mg and contains less than 45% Si. Peridotite can be found in xenoliths (rock fragments) brought to the surface by magma deriving from the upper mantle. Pl = plagioclase–$CaAl_2Si_2O_8$; Sp = spinel–$MgAl_2O_4$; Gt = garnet–$(Mg,Fe,Ca)_3Al_2Si_3O_{12}$; majorite garnet–$Mg_3(Mg,Si)_2Si_3O_{12}$; Cpx = clinopyroxene–$(Ca,Fe,Mg)SiO_3$; Opx = orthopyroxene–$(Mg,Fe)SiO_3$; Mg-Pv = Mg-perovskite–$(Mg,Fe)SiO_3$; olivine–$(Mg,Fe)_2SiO_4$; Mw = magnesiowüstite–$(Mg,Fe)O$; Ca-Pv = Ca-perovskite–$CaSiO_3$; St = stishovite–$SiO_2$.

ocean and 35 km beneath continents. We know that the crust consists mainly of rocks known as silicates, containing silicon and oxygen in tetrahedral form.

Beneath the crust lies the silicate mantle reaching a depth of 2890 km. The mantle can be divided into the upper and lower parts. The upper mantle is dominated by the minerals olivine, garnet and pyroxene (see figure 1). We know this because upper mantle rocks are sometimes brought to the surface either as huge (km scale) tectonic fragments or as small (cm scale) inclusions in volcanic rocks. Between the upper and lower mantles lies a transition zone extending from 410 to 660 km. This is bounded by two major global seismic wave discontinuities (depicted in figure 2). High-pressure experiments on upper mantle material reveal that the minerals present in the upper mantle transform to denser phases over a relatively narrow pressure interval corresponding to the pressures and temperatures found in the transition zone and thereby provide a potential explanation for these discontinuities (Liu 1979; Ringwood 1979) (see table 1).

$(Mg,Fe)SiO_3$-perovskite and $(Mg,Fe)O$-magnesiowüstite are believed to be the dominant and stable minerals of the lower mantle. Also present are

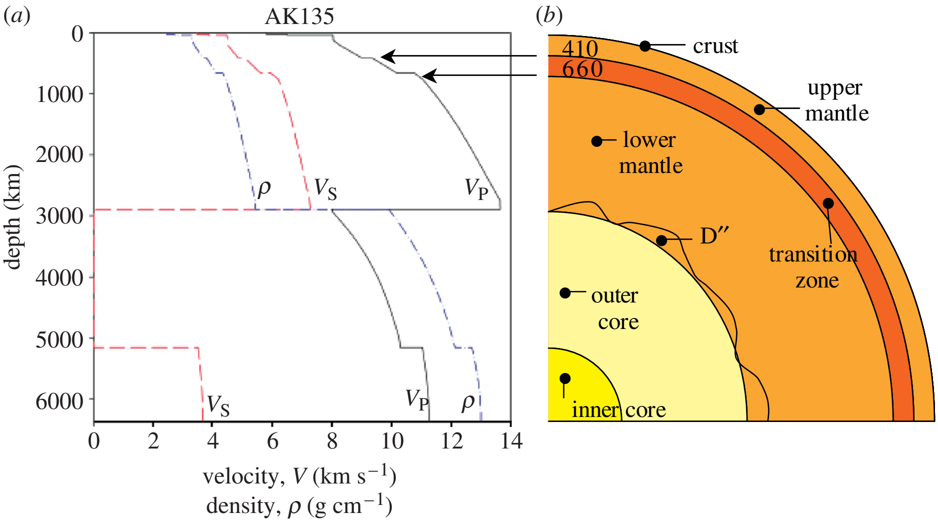

Figure 2. (*a*) Seismic and density structures of the lower mantle showing the major discontinuities at 410 and 660 km depth. (*b*) A cut-away model of the Earth. AK135 Earth model is taken from Kennett *et al.* 1995 (after Helffrich & Wood 2001).

Table 1. *Mineral transformations in the transition zone as depth increases (after Helffrich & Wood 2001)*

$(Mg,Fe)_2SiO_4$ olivine	⇒	$(Mg,Fe)_2SiO_4$ wadsleyite (β-spinel)	pressure, 13–14 GPa; depth, 410 km
$(Mg,Fe)_2SiO_4$ wadsleyite (β-spinel)	⇒	$(Mg,Fe)_2SiO_4$ ringwoodite (γ-spinel)	pressure, 18 GPa; depth, 520 km
$(Mg,Fe)_2SiO_4$ ringwoodite (γ-spinel)	⇒	$(Mg,Fe)SiO_3$ + $(Mg,Fe)O$ perovskite magnesiowüstite	pressure, 23 GPa; depth, 660 km

$CaSiO_3$-perovskite and SiO_2-stishovite (plus Al and water components). The bottom 200 km of the lower mantle (known as the D″ region) is characterized by a region of low-seismic-velocity structures and regional discontinuities (Lay *et al.* 1998). This area also exhibits anisotropy attributed to either alignment of crystals or compositional layering (Hall *et al.* 2004; Garnero *et al.* 2004). The interpretation of these features, in terms of a thermal and chemical structure, is an area under continuous development. Although we can place constraints on the composition of the lower mantle as a whole, we do not know the exact mineral compositions, their relative proportions or the state or quantities of any other minerals or elements that might be present.

Beneath the mantle lies the core. The core is believed to consist mainly of iron and nickel with some other lighter elements, potentially Co, Cr, Mn, Si, O and/or S (see Wood (1993) and Poirier (1995) for a discussion of light elements in the core). Again, the core can be subdivided into two sections. The liquid outer core reaches to a depth of 5150 km while the solid inner core reaches to a depth of 6371 km. The exact chemical and physical composition of the core is also unknown, but that is a discussion for another article!

3. The problem in terms of mineral physics

In order to interpret the observed density and seismic structures of the lower mantle (see figure 2) in terms of its composition, accurate descriptions of the seismic velocities and thermodynamic properties of the candidate materials are required. During the last 30 years, considerable effort has been expended to find the physical and chemical properties of lower mantle minerals, both at ambient conditions and at high pressures and temperatures. It has been difficult, however, to get complete internally consistent sets of thermodynamic properties for these minerals because the experimental procedures for measuring these properties at high pressures and temperatures are very complex. Differences in the values of the parameters lead to a whole range of contrasting compositional models with vastly different implications for the evolution of the Earth.

The basic thermodynamic properties that describe mineral behaviour include:

(i) the mineral *equations of state* (descriptions of the volume, V, of the mineral at various pressures, P, and temperatures, T);
(ii) the *coefficient of thermal expansivity*, α (a measure of the change in V resulting from a change in T at constant P);
(iii) the *bulk modulus*, K (stiffness, i.e. the parameter that relates the mean normal stress to the volumetric strain—in other words, it is the relationship between the hydrostatic pressure (the stress consisting of uniform pressure in all directions) and the change in volume or density);
(iv) the *shear modulus*, G (rigidity, i.e. the parameter that relates the shear stress at a point in a body to shear strain—in other words G refers to the change of shape produced by a tangential stress);
(v) other *elastic constants*, C_{ij} (that relate to the stress and strain acting on a mineral plane in a particular direction and can also be derived as the second derivatives of the lattice energy with respect to the strain components);
(vi) and the *seismic velocities* (the speeds of the compressional, V_P, and shear, V_S, seismic waves through the minerals).

K, G, V_P, V_S and the density, ρ, are used to link the observed seismic structure of the Earth with potential compositions. In an infinite material, V_P and V_S are described by the appropriate elastic modulus divided by the density of the material. A further parameter, Φ, the seismic parameter, links K to ρ:

$$V_\mathrm{P} = \left(\frac{K + \frac{4}{3}G}{\rho}\right)^{1/2}, \quad V_\mathrm{S} = \left(\frac{G}{\rho}\right)^{1/2}, \quad \Phi = \left(\frac{K}{\rho}\right). \tag{3.1}$$

Traditionally, comparisons of compositional models with seismological models have been made using only bulk modulus and density. The shear modulus and sound velocities have been excluded because of the difficulties inherent in obtaining reliable estimates of these parameters. Unlike the bulk modulus, the shear modulus has no thermodynamic expression so it can be derived only experimentally or from the elastic constants and their derivatives, but these are even harder to obtain. Calculations of sound velocities are possible, but they involve the elusive shear modulus (see equations (3.1)). (See Pollard (1977) and Nye (1985) for basic elasticity theory and Barron & Klein (1965), Wallace (1970) and Stixrude (2000) for more specific texts).

As previous work has shown (e.g. Zhao & Anderson 1994), models based only on the bulk modulus and density do not provide sufficiently strong constraints to differentiate between different mantle models. Accurate descriptions of the elastic properties and velocities of mantle minerals are, therefore, essential for understanding and interpreting the Earth's seismic profile. Recent advances have gone some way towards alleviating this problem, and current lower mantle models are based on all of these parameters.

4. Improvements in experimental and computational mineralogy

Experimental and analytical techniques have seen significant improvements in recent years (Fiquet *et al.* 2004; Li *et al.* 2004*a*), and the elastic properties essential for linking mineralogical models to observed seismic and density data can now be measured at high pressures and temperatures using a variety of different techniques (see table 2).

Although these methods provide valuable data, experiments have not yet been carried out on all the possible mantle phases, and none of these methods provide detailed enough measurements of the elastic properties or velocities of minerals at the pressures or temperatures found in the lower mantle.

Fortunately, complementary to these experimental techniques, computational methods have also advanced by leaps and bounds. These techniques are important for investigating the structural and dynamical properties of matter at an atomic level. They help us to understand the fundamental physics behind experimental observations and they help us to probe the properties of minerals at the high P/T conditions not currently accessible by experimental techniques. In addition, sets of self-consistent thermodynamic parameters can be derived from such methods, which can then be used to derive consistent mantle models.

Broadly, these techniques involve either finding the solution to the Schrödinger wave equation to calculate the total energy of the mineral species by quantum mechanical techniques or the use of an interatomic potential model to describe atomic interactions as a function of atomic separation and geometry.

Bonding between atoms in a mineral is usually discussed in terms of molecular orbital theory, which describes the way electrons interact with nuclei to form molecules. The assumption is that electrons have wave-like properties that can be described by wave functions that result from the interactions of the electrons with all the nuclei in the molecule. The Schrödinger equation is used to calculate the wave function. It is the fundamental equation in wave mechanics.

Quantum mechanical first principles (or *ab initio*) methods may employ either Hartree–Fock techniques or density functional theory (DFT). (See Catlow *et al.* (1994), Price & Vocădlo (1996) and Brodholt *et al.* (2002) for a full review.)

The Hartree–Fock approach involves setting up and solving the Hartree–Fock equations for a particular system, in a self-consistent manner. The problem cannot usually be solved analytically owing to the complexity of the equations

Table 2. *High pressure and/or temperature experiments on the elasticity of mantle minerals*
(Note that atmospheric pressure is approximately 1 bar = 100 000 Pa; 10 kilobars = 1 GPa; 0 °C = 273.15 K. The lower mantle pressure range is from *ca* 23 to 135 GPa and the temperature range is from *ca* 1900 to 4000 K.)

method	material	P (GPa)	T (K)	references
ultrasonic interferometry (GHz)	MgO	6	523	Bassett *et al.* (2000)
	Magnetite	8.7		Reichmann & Jacobsen (2004)
	(Mg,Fe)O	9.1		Jacobsen *et al.* (2004)
	Polycrystalline olivine		1300	Jackson *et al.* (2005)
ultrasonic interferometry	$MgSiO_3$-garnet	8		Gwanmesia *et al.* (1998)
	pyrope	10		Chen *et al.* (1999)
	$MgSiO_3$-orthopyroxene	10		Flesch *et al.* (1998)
	wadsleyite	10		Li & Liebermann (2000)
shock-compression	fosterite	150		Duffy & Ahrens (1992)
	MgO	27		Duffy & Ahrens (1995)
Brillouin spectroscopy and X-ray diffraction	MgO		2500	Sinogeikin *et al.* (2004)
	MgO	55		Zha *et al.* (2000)
	MgO and pyrope	20		Sinogeikin & Bass (2000)
radial X-ray diffraction	iron	220		Mao *et al.* 1998
inelastic X-ray scattering	iron	110		Fiquet *et al.* 2001
ultrasound spectroscopy	MgO		1800	Isaak *et al.* 1989
ultrasonic interferometry using a 1000 tonne uniaxial split-cylinder	MgO	8	1600	Chen *et al.* (1998)
	polycrystalline olivine	10	1300	Li *et al.* (1998)
	wadsleyite	7	873	Li *et al.* (2001)
	$MgSiO_3$-perovskite	8	800	Sinelnikov *et al.* (1998)

involved in even simple systems, so the problem is usually solved numerically by iteration. (Alternatively, semi-empirical techniques may be used where the integrals are parameterized from empirical data or set to zero.) Initially, a set of one-electron orbitals is required. An atomic orbital describes the region in which an electron is likely to be found in an atom and is determined by its total energy and its angular momentum. For a single atom, the orbitals are usually those of an atom with only one electron, but with the appropriate nuclear charge. For a molecule, atomic orbitals are typically combined linearly to give rise to a set of one-electron wave functions (the linear combination of atomic orbital formalism). In this approach the Born–Oppenheimer approximation is used in which the nuclei are considered fixed, although the true wave function is a function of the coordinates of each of the nuclei as well as the electrons. Once the wave functions are created, each electron is selected in turn, and a potential is generated for that electron that takes into account the effects of all the remaining electrons. The Schrödinger equation is then solved for that potential giving rise to a new wave function for that electron. The whole procedure is then repeated for every electron until convergence is reached.

Hartree–Fock had been the traditional approach of quantum chemistry and solid-state physics since the 1930s, until the approximations used in DFT were greatly refined in the 1990s. Unlike the Hartree–Fock theory, which is based on the complicated many-electron wave function, DFT uses electron density as the basic quantity. Electron density is a measure of the probability of an electron being present at a specific location. DFT involves a single electron moving in an averaged effective force field represented by a potential energy being created by the other electrons. The atomic nuclei are still considered fixed. Usually, the Kohn–Sham equations (Kohn & Sham 1965) are solved. These equations are exact in principle; however, the exact form of the many-body term (the 'exchange-correlation functional') is not known. (See Brodholt *et al.* (2002) for a discussion of exchange-correlation.) In practice, therefore, approximations to this term are made. The Kohn–Sham equations are solved using one of two methods. The local density approximation (LDA) (Lundqvist & March 1983) defines the exchange-correlation as a function of electron density at a given position, whereas the generalized gradient approximation (GGA) (Perdew *et al.* 1996) defines the exchange-correlation as a function of both the local electron density and the magnitude of its gradient. Compared with the Hartree–Fock method, DFT has lower computational costs.

As an alternative, a pseudopotential method (Pickett 1989) may also be used within the LDA. Here, a potential is used to describe the interactions of the valence electrons with the core electrons thereby reducing the number of electrons dealt with explicitly. (A valence electron is an electron in an outer shell of an atom that can participate in forming chemical bonds with other atoms.) This has the advantage of minimizing computational overheads at the cost of additional approximations.

All of these calculations are computationally expensive so they have usually been restricted to materials at zero temperature (the 'athermal limit'). Other methods exist, however, that deal with thermal properties. Traditional molecular dynamics (MD) can deal with the effect of temperature by numerically solving Newton's equations of motion on an atomistic scale to obtain information about its time-dependent properties. The method usually employs predefined potentials based on empirical data or on independent calculations of electronic structure. Recently, *ab initio* MD techniques have been developed in response to the increase in available computing power (see Marx & Hutter (2000) for a complete review). The basic difference between traditional MD and *ab initio* MD is that *ab initio* MD calculates the forces acting within the atoms with a first-principles calculation at every time-step as the MD trajectory is generated. In this way, the variables of the potential are not fixed but are considered as active degrees of freedom. The focus of the approximation is, therefore, shifted from selecting an appropriate potential to selecting a particular level of approximation for solving the Schrödinger equations. Although the method is relatively quick, it is still computationally expensive and thus restricted to a few hundred atoms.

Much less demanding calculations in the form of lattice dynamical models can also be used with predefined potentials. These methods are quick and easy and can simulate large systems at any pressure and temperature. However, it is difficult to derive sets of empirical potentials that correctly describe the atomic interactions.

As with any computational methods, assumptions and uncertainties mean that comparisons must be made with available experimental data and that judgment must be used to assess whether the calculations have achieved the

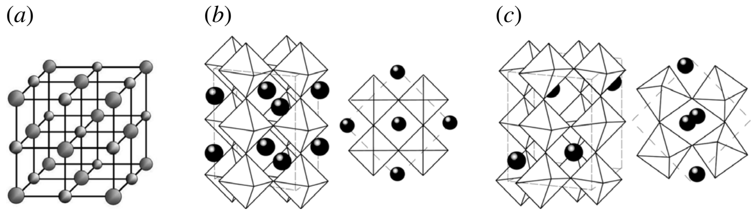

MgO-magnesiowüstite

$CaSiO_3$-perovskite (side and plan views)

$MgSiO_3$-perovskite (side and plan views)

Figure 3. Lower mantle mineral structures. (*a*) MgO-magnesiowüstite has a simple B1 or NaCl (salt) cubic structure with two atoms per unit cell, each occupying equivalent octahedral sites (Mao & Bell 1979; Fei 1999). (*b*) $CaSiO_3$-perovskite adopts a cubic structure with *Pm3m* space group symmetry (Wang *et al.* 1996). The lattice consists of a framework of corner-linked SiO_6 octahedra with the Si ion in the centre, located in the corners of a cube surrounding the central Ca ion (black ball), which is dodecahedrally coordinated with O. There are five atoms in a unit cell. (*c*) $MgSiO_3$-perovskite adopts an orthorhombic structure with *Pbnm* space group. There are four formula units and 20 atoms per unit cell. Like $CaSiO_3$, the lattice consists of a framework of corner-linked SiO_6 octahedra. These are nearly perfectly rigid (Horiuchi *et al.* 1987; Ross & Hazen 1990). Mg (black ball) resides in the dodecahedral cavities of the framework, coordinated with eight near-neighbour and four more distant O. In the orthorhombic structure, the octahedra are rotated around the Si ions, and the Mg ions are displaced. Structural refinements have shown an increase in orthorhombic distortion with increasing pressure, counterbalanced by a decrease in distortion at high temperatures (Fiquet *et al.* 2000). (Diagrams modified after Warren *et al.* (1998).)

accuracy required for a particular need. Bearing in mind these limitations, computational methods provide an excellent means of predicting properties of minerals that are otherwise unavailable experimentally at present.

5. Elastic properties of lower mantle minerals

The lower mantle is believed to be mainly composed of the elements O, Mg, Si, Fe, Al and Ca (Ringwood 1975) accommodated within the minerals (Mg,Fe)SiO_3-perovskite; (Mg,Fe)O-magnesiowüstite (also known as periclase); $CaSiO_3$-perovskite and SiO_2-stishovite. Although Al is believed to constitute about 4–5 wt% of the lower mantle (Ringwood 1975), its host is still uncertain. It may reside within the (Mg,Fe)SiO_3-perovskite phase (at pressures above 26 GPa) (Irifune 1994; Irifune *et al.* 1996) or it may form a separate phase (Kesson *et al.* 1995; Oganov & Brodholt 2000).

Experimental work has traditionally been carried out on the pure end-member minerals $MgSiO_3$ and MgO (see figure 3) for simplicity as they are easier to prepare experimentally and to study theoretically than the mixed Mg–Fe phases. Comparisons between the experimental and theoretical elastic constants of these minerals are shown in figure 4.

$CaSiO_3$-perovskite forms a separate phase under lower mantle conditions (Liu & Ringwood 1975; Tamai & Yagi 1989; Oguri *et al.* 1997). It is potentially the third most abundant mineral, constituting between 6 and 12 wt% of the lower mantle (Ringwood 1975; Bass & Anderson 1984; Anderson 1989*b*). It remains stable in a dense cubic phase (see figure 3) over a wide range of mantle pressures and temperatures (Mao *et al.* 1989; Wang *et al.* 1996; Shim *et al.* 2000*a*,*b*).

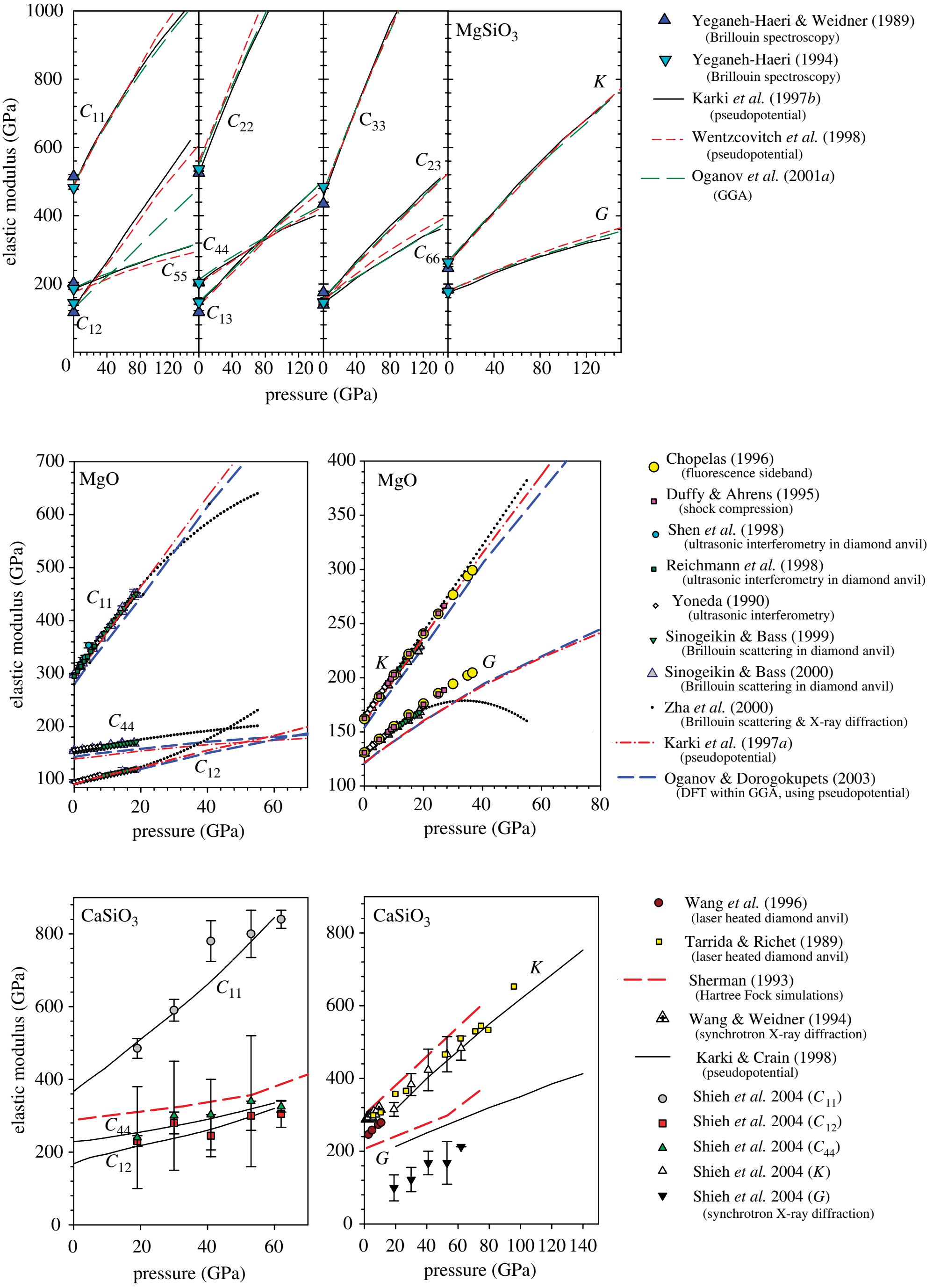

Figure 4. Elastic constants (C_{ij}) and elastic moduli (K and G) for the three main lower mantle minerals: $MgSiO_3$-perovskite, MgO-magnesiowüstite and $CaSiO_3$-perovskite. Lines are theoretical calculations. Points are experimental data.

Measurements of its thermal properties at ambient conditions are difficult, however, because the cubic phase is dynamically unstable at low P/T and it transforms readily to glass on release of pressure after quenching from high temperature (Liu & Ringwood 1975). Data on the elastic properties of $CaSiO_3$ are, therefore, scarce and scattered (see figure 4).

6. The effects of Fe

Although studying pure $MgSiO_3$ and MgO gives us a broad understanding of the thermodynamic properties of (Mg,Fe)SiO_3-perovskite and (Mg,Fe)O-magnesiowüstite, it cannot be assumed (as it has been in the past) that the incorporation of Fe into the structures only increases the mineral mass. The substitution of Fe for other atoms such as Mg normally leads to an increase in the mineral mass but also leads to changes in the lattice caused by the differences in atom size, which may then lead to changes in the thermodynamic properties.

The lattice of $MgSiO_3$-perovskite is somewhat distorted as shown in figure 3. The addition of 10 or 20% Fe to perovskite has been shown to decrease the distortion of the unit cell slightly (O'Neill & Jeanloz 1994) and to have only a minor effect on the bulk modulus and its derivatives (Mao *et al.* 1991; Anderson & Hama 1999). The effect on the shear modulus is uncertain, but the addition of Fe is believed to decrease it perhaps by as much as 6–8% (Kiefer *et al.* 2002).

There are also limited data on magnesiowüstite. The FeO end-member is non-stoichiometric, which means that the elements do not combine in simple whole-number ratios, although the pure composition can be approached closely at high pressure (Fei & Saxena 1986) and non-stoichiometry decreases with increasing Mg content (see Fei *et al.* 1991). Its non-stoichiometry and porosity and the use of different experimental methods and conditions have meant that experimental values for the bulk modulus of FeO have been rather scattered with values ranging from 141.5 to 185 GPa (Bonczar & Graham 1982; Jackson *et al.* 1990; Stølen & Grønvold 1996; Fei 1999). These different results have made it difficult to establish the effects of increasing Fe content on the value of the bulk modulus. Although some believe that the bulk modulus is independent of iron content, others believe that even a small amount of iron has a significant effect (see figure 5).

The elastic constant, C_{11}, which affects both K and G, has been shown to decrease significantly with increasing Fe content except near pure MgO where a small amount of Fe leads to an increase in C_{11} (Reichmann *et al.* 2000). This suggests that the elastic behaviour of the magnesiowüstite changes considerably, and nonlinearly, with increasing Fe content (see also Jacobsen *et al.* 2004). The shear modulus of magnesiowüstite is already known to decrease with increasing Fe content (see figure 5).

While MgO has been found to be stable up to 227 GPa (Duffy *et al.* 1995), the high-pressure behaviour of FeO is quite different. At about 16 GPa, FeO distorts from the B1 (NaCl) structure into a rhombohedral cell (Kondo *et al.* 2004). A further transition to a B8 (NiAs structure) phase has been proposed above 90 GPa (Mao *et al.* 1996). However, conflicting results have been found at different pressures and high temperatures (Fei & Mao 1994; Lin *et al.* 2003,

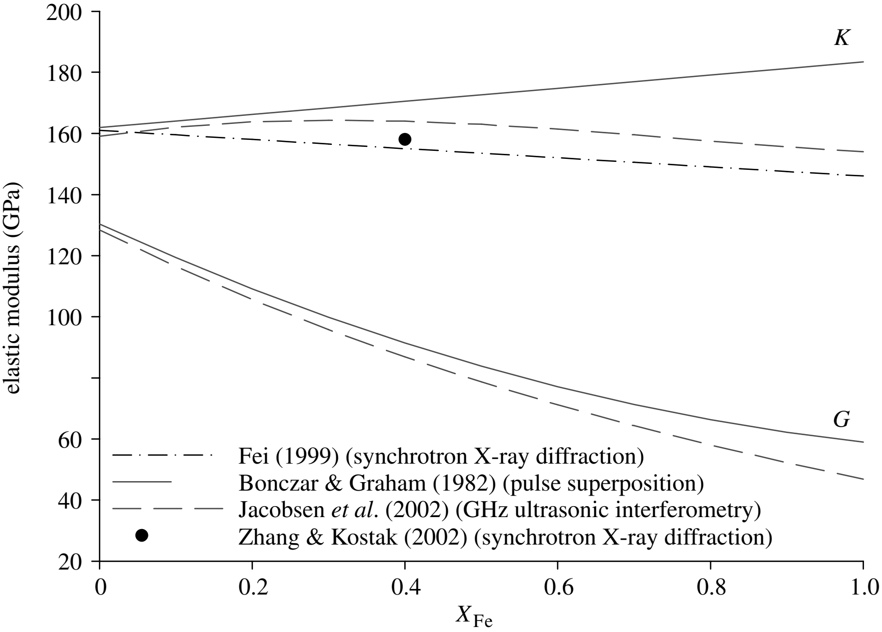

Figure 5. The variation of the bulk (K) and shear (G) moduli with iron content [$X_{\mathrm{Fe}}=\mathrm{Fe}/(\mathrm{Mg}+\mathrm{Fe})$] for (Mg,Fe)O-magnesiowüstite under ambient conditions. (Pure MgO is on the left of the x-axis)

see also Jacobsen *et al.* 2004). The stable phase of Fe-bearing (Mg,Fe)O at temperatures and pressures typical of the lower mantle is, therefore, still unclear.

7. Partitioning of Fe between perovskite and magnesiowüstite

In a simple system of MgO–FeO–SiO_2, iron preferentially partitions into (Mg,Fe)O-magnesiowüstite instead of into (Mg,Fe)SiO_3-perovskite (Ito *et al.* 1984; Katsura & Ito 1996). This partitioning is usually discussed in terms of the partition coefficient, k. The partition coefficient of Fe and Mg between perovskite and magnesiowüstite is defined by $k=(X_{\mathrm{Fe}}^{\mathrm{Pv}}/X_{\mathrm{Mg}}^{\mathrm{Pv}})/(X_{\mathrm{Fe}}^{\mathrm{Mw}}/X_{\mathrm{Mg}}^{\mathrm{Mw}})$ where X is the mole fraction of Fe or Mg (i.e. FeO/(MgO+FeO) and MgO/(MgO+FeO), respectively) in perovskite or magnesiowüstite. The value of k is still uncertain. It varies from about 0.09 to 0.29 depending on the pressure, temperature and initial composition (see Mao *et al.* 1997); k increases with increasing P, increasing T, decreasing ferrous iron (Fe^{2+}) content and increasing ferric iron (Fe^{3+}) content (Mao *et al.* 1997). Since P and T increase along the mantle geotherm, k will increase with depth if the lower mantle has a constant bulk composition; more Fe would, therefore, reside in perovskite rather than magnesiowüstite with increasing depth.

On the basis of this three-component system, the lower mantle is believed to consist of mainly (Mg,Fe)SiO_3-perovskite, with about 20% (Mg,Fe)O-magnesiowüstite.

8. The effects of Al

It is already known that in the presence of aluminium the behaviour of (Mg,Fe)SiO_3 changes so that, although iron tends to destabilize (Mg,Fe)SiO_3, in the presence of Al_2O_3 the stability field of Mg-perovskite is extended towards iron-rich compositions (Kesson *et al.* 1995; Wood & Rubie 1996).

The addition of iron and/or aluminium results in an increase in the size of the $MgSiO_3$-perovskite unit cell (O'Neill & Jeanloz 1994; Kesson *et al.* 1995; Walter *et al.* 2004). Fe leads to a slight decrease in the distortion of the unit cell whereas Al significantly increases the distortion. Unlike substitution of Fe, the substitution of Al could also result in a decrease in the bulk modulus (Kesson *et al.* 1995; Liu *et al.* 1995; Zhang & Weidner 1999; Walter *et al.* 2004; Yagi *et al.* 2004; Daniel *et al.* 2004).

The incorporation of Al_2O_3 into $MgSiO_3$, therefore, would increase the volume, decrease the density and decrease the bulk modulus of silicate perovskite depending on the FeO and Al_2O_3 concentrations. These results are still being challenged, however, (Andrault *et al.* 2001) and may depend on factors involved in the choice of experimental technique (Yagi *et al.* 2004). The shear modulus is also predicted to decrease (Jackson *et al.* 2004). This would lead to changes in the wave velocities of silicate perovskite and would, therefore, affect compositional models.

The occurrence of Al in perovskite also affects the inherent behaviour of Fe, such as whether it is present in its ferrous or ferric state (McCammon 1997) and whether it takes a high- or low-electronic spin state (Li *et al.* 2004*b*). The spin state affects the magnetic susceptibility of its host and the Fe ionic radius (and hence the volume of the material) and may also affect separations between Fe-rich and Mg-rich phases. This, in turn, would have an important bearing on the magnetic, thermoelastic and transport properties of the lower mantle and the distribution of iron in the Earth's interior (Li *et al.* 2004*b*).

The presence of Al_2O_3 would also affect the partitioning of Fe and Mg between perovskite and magnesiowüstite, perhaps increasing the partition coefficient with increasing Al_2O_3. This, in turn, would affect the relative densities of the materials and hence the overall properties of the mix.

9. Lower mantle models

Uncertainties in the elastic properties of lower mantle minerals as functions of temperature, pressure and composition mean that there are several possible combinations of mineral structures and compositions that match the observed data. Each model has different and significant implications for the evolution and current state of the Earth.

Very simply, the Earth is widely accepted to have been formed by the accumulation of planetismals (small planet-like bodies). The composition of these would have been similar to that of chondritic meteorites, themselves having derived from the solar nebula. As the Earth cooled, heavier elements, such as iron, settled towards the centre of the Earth forming the core, and lighter elements, such as magnesium and oxygen, were pushed upwards forming the primitive mantle in a process known as differentiation (see Ahrens (1990), O'Neill (1991), Javoy (1999) and Walter & Trønnes (2004) for more detailed reviews). The question is to what extent did the primitive mantle differentiate? We assume that the Earth has a chondritic bulk composition (having been assembled from chondritic material). We also know the present composition of the upper mantle relatively well; therefore, if in the past the crust was formed exclusively from the upper mantle, a mass-balance calculation tells us that the lower mantle would have to be richer in silicon, and perhaps iron, and have a lower Mg/Si ratio than the upper mantle in order to match the chondritic bulk Earth composition. This scenario gives rise to 'chondritic' lower mantle models (Anderson 1984, 1989*a*; Jeanloz & Knittle 1989; Bina & Silver 1990, 1997; Zhao & Anderson 1994). The upper and lower mantle would, therefore, have different compositions.

The upper mantle has a high Mg/Si ratio relative to chondritic meteorites. This is another long-standing mystery that cannot yet be explained satisfactorily. Perhaps the bulk Earth composition is not chondritic after all, or perhaps the composition of the Earth's mantle has changed over time and a Si-rich reservoir exists somewhere within the mantle. Kellogg *et al.* (1999), for example, suggest that a compositionally distinct and, therefore, isolated region may exist in the bottom 1000 km of the mantle (see also Francis 2003). Other geochemical arguments also favour a broadly chondritic lower mantle composition; e.g. there is an excessive abundance of siderophile (or iron-loving) elements in the mantle, which should be present only in small proportions owing to their highly fractional nature (see Li & Agee 1996; Kesson *et al.* 1997).

On the other hand, if the entire primitive mantle was involved in the formation of the crust, then the lower mantle would have the same composition as the upper mantle (pyrolite) and the whole mantle would be homogeneous. This scenario gives rise to 'pyrolitic' models (Ringwood 1979; Jackson & Rigden 1998; Jackson 1998; Fiquet *et al.* 1998; Hama & Suito 2001; Marton & Cohen 2002). Other models also exist however (e.g. Fiquet *et al.* 2000; Lee *et al.* 2004). For example, it has been shown that the lower mantle could be made exclusively from perovskite (Stixrude *et al.* 1992), and this list is by no means exhaustive.

10. Mantle mixing

The main debate is focused on the exact nature of the transition zone. Can the presence of the 660 km discontinuity, which divides the upper mantle from the lower mantle, be solely explained by the changes that occur in mineral structure owing to increased pressure, or do differences in chemical composition also exist? The 660 km discontinuity corresponds to the spinel–perovskite transition (see figure 1 and table 1) so there is no need to invoke a chemical change, although this does not imply that a chemical change does not exist.

The nature of the transition zone affects convection models. If the 660 km discontinuity is a total barrier to convection, then separate convective systems must exist above and below, and the mantle is likely to be heterogeneous. Seismic data suggest that while some subducting slabs are deflected by the 660 km discontinuity (suggesting that the slab encounters resistance) others penetrate this barrier (e.g. Widiyantoro *et al.* 1999; van der Hilst & Karason 1999; Collier *et al.* 2001; Shito & Shibutani 2001; Thomas *et al.* 2004) (see figure 6). The low

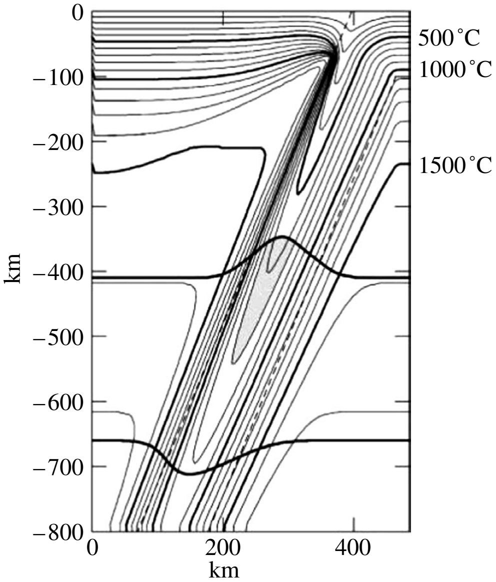

Figure 6. Thermal model of the Izu-Bonin subducting slab. The diagram shows the penetration of the lower mantle by the steeply dipping subducting slab. This is indicated by the depression of the 660 km discontinuity. The 410 km discontinuity is elevated, implying a thermal anomaly of approximately 900–1000 °C relative to the ambient mantle. Seismic observations show that the olivine to wadsleyite phase transformation occurs under essentially equilibrium conditions there. (Reproduced with kind permission of G. R. Helffrich, from Collier *et al.* 2001).

thermal anomalies usually interpreted as slabs penetrating into the lower mantle could also, however, be explained as the result of cooling from the subducting slab, which remains in the upper mantle (Cizkova *et al.* 1999). Perhaps the slabs penetrating into the lower mantle and the elastically distinct bodies found in the lower mantle point towards a lower mantle that has lateral chemical heterogeneities rather than radial ones (Helffrich 2002). (See Davies *et al.* (2002) for a review.)

Compositional layering at the 660 km discontinuity would require thermal boundary layers above and below the boundary. Recently, Oldham & Davies (2004) showed the scale of the temperature and density contrasts that would be required for a stratified layered mantle. These are large. Since no seismic reflectors were found around the mid-mantle zone (Vidale *et al.* 2001), this is a further argument against mantle layering.

11. Seismic tomography

Seismic tomography is the geophysical analogue of a medical CAT scan and is used to determine a three-dimensional pattern of seismic wave velocities in the Earth. Tomographic models reveal fast and slow seismic velocity anomalies, which are usually interpreted as representing a spatially heterogeneous temperature field associated with mantle convection. This is because waves will propagate faster in hot less dense regions such as 'hot spots' and propagate slower in cold denser regions such as in a subducted slab.

Global tomographic models of the Earth (Ekström & Dziewonski 1998; Masters *et al.* 2000) can provide good-quality maps of lower mantle velocities. Unfortunately, their interpretation is difficult because knowledge of the lower mantle composition, pressure and temperature are required. Nonetheless, attempts have been made to interpret these tomographic maps by extrapolating mineral physics data from ambient conditions to lower mantle pressures and temperatures (Forte & Mitrovica 2001).

12. The lateral correlation of V_{P} and V_{S} in the lower mantle

Compressional- and shear-wave velocity anomalies have been found to have unexpected correlations and anti-correlations at particular depths (e.g. Inoue *et al.* 1990; Trampert *et al.* 2004). A parameter, $R_P = (\partial \ln V_{\mathrm{S}}/\partial \ln V_{\mathrm{P}})_P$, relates V_{S} to V_{P} at a particular pressure. The value of R_P within these anomalies is observed to be greater than 1. At a given depth, this implies that any variation in V_{P} is matched by a greater variation in V_{S}. Using equation (3.1), it can thus be inferred that the lateral variation in shear modulus is greater than the lateral variation in bulk modulus.

In the lower mantle, R_P has been found to increase from about 1.7 to more than 3 at depths of 2000 km (Woodhouse & Dziewonski 1989; Robertson & Woodhouse 1996). These seismic anomalies are not easy to reconcile with mineral physics data, which indicate that R_P for lower mantle minerals lies between 1.4 and 1.9 (but could be as high as 2.5) at pressures and temperatures typical of the lower mantle (Isaak *et al.* 1992; Karki & Stixrude 1999; Karki *et al.* 1999; Oganov *et al.* 2001*b*).

Several explanations for the large values of R_P observed in the lower mantle have been put forward. Lateral variations of V_{P} and V_{S} in the lower mantle can be explained as being solely caused by temperature fluctuations. However, this requires a surprisingly large negative shear modulus temperature derivative $(\partial G/\partial T)_P$ of -0.030 to -0.043 (Anderson *et al.* 1987; Wang & Weidner 1996; Jackson 1998). Since perovskite is thought to be the most abundant lower mantle mineral, this would mean that the high pressure and temperature $(\partial G/\partial T)_P$ for perovskite would also be an anomalously large negative value.

To try and reconcile mineral physics data with the observed lower mantle properties, a separate theory based on anelastic effects has also been put forward (Karato 1993; Karato & Karki 2001; Oganov *et al.* 2001*b*). Anelastic effects are those in which there is a time delay between the strain and the imposed stress (i.e. the strain is dependent on both stress and time). These effects are not usually measured in experiments performed at high laboratory frequencies (*ca* 1 MHz) but do affect measurements of low seismic wave frequencies (less than 1 Hz) in the Earth. Anelasticity affects the shear modulus more than the bulk modulus and hence shear-wave velocity more than compressional-wave velocity. Experimentally determined values of R_P would, therefore, be lower than those measured in the Earth. There is strong evidence, however, that anelasticity does not contribute to the observed wave speeds in the lower mantle. First, the lower mantle is not significantly attenuating (in fact it is the second best transmitter of seismic waves after the outer core). Second, if there were an anelastic contribution to wave speeds, then body waves would be dispersive, and observationally they are not (G. R. Helffrich 2002, personal communication). Therefore, anelasticity is probably not responsible for the observed discrepancies.

The large lateral variation in the shear modulus of the lower mantle must therefore be the result of other causes, such as a lateral variation in chemical composition (Kennett *et al.* 1998; Ishii & Tromp 1999; Trampert *et al.* 2004). This could be caused by Fe content (Weidner & Zhao 1992; Zhao *et al.* 1994) or Si content (see Bina 1998) or even Al_2O_3 or CaO. Variations in the partitioning of Fe between perovskite and magnesiowüstite could occur because of convective mixing or differences in lateral differentiation processes caused by partial melting early in the Earth's history (see Karato & Karki 2001 and references therein). Areas that have undergone higher degrees of partial melting usually have lower Fe/(Fe+Mg) and higher Si/(Si+Mg) ratios.

Phase transformations could also be responsible. Recently, a post-perovskite phase has been discovered (Murakami *et al.* 2004; Oganov & Ono 2004; Iitaka *et al.* 2004) whose elastic properties may help explain the origin of the D$''$ seismic discontinuity. Several processes or combinations of processes could, therefore, be responsible for this phenomenon and research is still ongoing.

13. Conclusion

From the exact nature of the transition zone, to the composition and structure of the most voluminous region of our Earth, to the mysterious D$''$ layer at the edge of the outer core, the lower mantle is an intriguing region of the Earth. Although we have to determine its properties remotely, we have already gained considerable insight into its structure and possible development, but there are many mysteries still to be solved.

Although there are several new developments and results in mineral physics, the current uncertainties in the thermodynamic and elastic properties of lower mantle minerals make it impossible to differentiate between current lower mantle compositional models.

Recent geophysical studies, such as traditional analyses of arrival time, seismic tomography and newer scattering studies, provide detailed images of the interior of the Earth, the deep mantle structure and its heterogeneities and so provide strong constraints on mantle models. However, further geochemical studies on minerals, rocks and melts are also required to help decipher the complexities of element partitioning and phase transitions of lower mantle materials.

The elastic properties and seismic wave velocities of mantle minerals are required to link the compositional models to the observed data. Improving our knowledge of these properties under the relevant conditions of high pressure and temperature should enable us to place tighter constraints on the lower mantle composition and its lateral heterogeneity. Further technological, analytical and computational advances will help us to achieve this aim. I look forward to this future work and hope that further research at both atomic and planetary scales will improve our knowledge of the Earth.

I thank Prof. George R. Helffrich, Prof. Dave M. Sherman and NERC for supporting this work, and I thank Prof. George R. Helffrich and Dr J. Huw Davies for their helpful comments on this manuscript.

References

Ahrens, T. J. 1990 Earth accretion. In *Origin of Earth* (ed. H. E. Newsom & J. H. Jones), pp. 211–227. Oxford: Oxford University Press, and Houston: Lunar & Planetary Institute.

Anderson, D. L. 1984 The Earth as a planet: paradigms and paradoxes. *Science* **223**, 347–355.

Anderson, D. L. 1989*a* Composition of the Earth. *Science* **243**, 367–370.

Anderson, D. L. 1989*b* *Theory of the Earth.* Oxford: Blackwell Scientific Publications.

Anderson, O. L. & Hama, J. 1999 Shifts in thermal expansivity with Fe content for solid solutions of $MgSiO_3$–$FeSiO_3$ with the perovskite structure. *Am. Mineral.* **84**, 221–225.

Anderson, O. L., Goto, T. & Isaak, D. 1987 The $\mathrm{dln}\,V_S/\mathrm{dln}\,V_P$ parameter in seismic tomography. *EOS Trans. Am. Geophys. Union* **68**, 1488.

Andrault, D., Bolfan-Casanova, N. & Guignot, N. 2001 Equation of state of lower mantle (Al,Fe)–$MgSiO_3$. *Earth Planet. Sci. Lett.* **193**, 501–508. (doi:10.1016/S0012-821X(01)00506-4.)

Barron, T. H. K. & Klein, M. L. 1965 Second-order elastic constants of a solid under stress. *Proc. Phys. Soc.* **85**, 523–532. (doi:10.1088/0370-1328/85/3/313.)

Bass, J. D. & Anderson, D. L. 1984 Composition of the upper mantle: geophysical tests of two petrologic models. *Geophys. Res. Lett.* **11**, 237–240.

Bassett, W. A., Reichmann, H. J., Angel, R. J., Spetzler, H. & Smyth, J. R. 2000 New diamond anvil cells for gigahertz ultrasonic interferometry and X-ray diffraction. *Am. Mineral.* **85**, 283–287.

Bina, C. R. 1998 Lower mantle mineralogy and the geophysical perspective. In *Ultrahigh pressure mineralogy, physics and chemistry of the Earth's deep interior*, vol. 37 (ed. R. J. Hemley). Reviews in Mineralogy, pp. 205–239. Washington DC: Mineralogical Society America.

Bina, C. R. & Silver, P. G. 1990 Constraints on lower mantle composition and temperature from density and bulk sound velocity profiles. *Geophys. Res. Lett.* **17**, 1153–1156.

Bina, C. R. & Silver, P. G. 1997 Bulk sound travel times and implications for mantle composition and outer core heterogeneity. *Geophys. Res. Lett.* **24**, 499–502. (doi:10.1029/97GL00353.)

Bonczar, L. J. & Graham, E. K. 1982 The pressure dependence of the elastic properties of polycrystal magnesiowüstite. *J. Geophys. Res.* **87**, 1061–1078.

Brodholt, J. P., Oganov, A. R. & Price, G. D. 2002 Computational mineral physics and the physical properties of perovskite. *Phil. Trans. R. Soc. A* **360**, 2507–2520. (doi:10.1098/rsta.2002.1078.)

Catlow, C. R. A., Bell, R. G. & Gale, J. D. 1994 Computer modelling as a technique in materials chemistry. *J. Mater. Chem.* **4**, 781–792. (doi:10.1039/jm9940400781.)

Chen, G., Liebermann, R. C. & Weidner, D. J. 1998 Elasticity of single-crystal MgO to 8 GPa and 1600 K. *Science* **280**, 1913–1916. (doi:10.1126/science.280.5371.1913.)

Chen, G., Cook, J. A., Gwanmesia, G. D. & Liebermann, R. C. 1999 Elastic wave velocities of $Mg_2Al_2Si_3O_{12}$-pyrope garnet to 10 GPa. *Am. Mineral.* **84**, 384–388.

Chopelas, A. 1996 The fluorescence side-band method for obtaining acoustic velocities at high compressions: application to MgO and $MgAl_2O_4$. *Phys. Chem. Miner.* **23**, 25–37. (doi:10.1007/BF00202990.)

Cizkova, H., Cadek, O., van den Berg, A. P. & Vlaar, N. H. 1999 Can lower mantle slab-like seismic anomalies be explained by thermal coupling between the upper and lower mantles? *Geophys. Res. Lett.* **26**, 1501–1504.

Collier, J. D., Helffrich, G. R. & Wood, B. J. 2001 Seismic discontinuities and subduction zones. *Phys. Earth Planet. In.* **127**, 35–49. (doi:10.1016/S0031-9201(01)00220-5.)

Daniel, I., Bass, J. D., Fiquet, G., Cardon, H., Zhang, J. Z. & Hanfland, M. 2004 Effect of aluminium on the compressibility of silicate perovskite. *Geophys. Res. Lett.* **31**, L15 608. AUG 5 2004. (doi:10.1029/2004GL020213.)

Davies, J. H., Brodholt, J. P. & Wood, B. J. 2002 Introduction. *Phil. Trans. R. Soc. A* **360**, 2361–2369. (doi:10.1098/rsta.2002.1086.)

Duffy, T. S. & Ahrens, T. J. 1992 Sound velocities at high pressure and temperature and their geophysical implications. *J. Geophys. Res.* **97**, 4503–4520.

Duffy, T. S. & Ahrens, T. J. 1995 Compressional sound velocity, equation of state, and constitutive response of shock-compressed magnesium oxide. *J. Geophys. Res.* **100**, 529–542. (doi:10.1029/94JB02065.)

Duffy, T. S., Hemley, R. J. & Mao, H. K. 1995 Equation of state and shear-strength at multimegabar pressures—magnesium-oxide to 227 GPa. *Phys. Rev. Lett.* **74**, 1371–1374. (doi:10.1103/PhysRevLett.74.1371.)

Dziewonski, A. M. & Anderson, D. L. 1981 Preliminary reference Earth model. *Phys. Earth Planet. In.* **25**, 297–356. (doi:10.1016/0031-9201(81)90046-7.)

Ekström, G. & Dziewonski, A. M. 1998 The unique anisotropy of the Pacific upper mantle. *Nature* **394**, 168–172.

Fei, Y. 1999 Effects of temperature and composition on the bulk modulus of (Mg,Fe)O. *Am. Mineral.* **84**, 272–276.

Fei, Y. & Mao, H. K. 1994 *In situ* determination of the NiAs phase of FeO at high pressure and temperature. *Science* **266**, 1668–1680.

Fei, Y. & Saxena, S. K. 1986 A thermochemical data base for phase equilibria in the system Fe–Mg–Si–O at high pressure and temperature. *Phys. Chem. Miner.* **13**, 311–324. (doi:10.1007/BF00308348.)

Fei, Y., Mao, H. K. & Mysen, B. O. 1991 Experimental determination of element partitioning and calculation of phase relations in the MgO–FeO–SiO_2 system at high pressure and temperature. *J. Geophys. Res.* **96**, 2157–2169.

Fiquet, G., Andrault, D., Dewaele, A., Charpin, T., Kunz, M. & Haüsermann, D. 1998 *P–V–T* equation of state of $MgSiO_3$ perovskite. *Phys. Earth Planet. In.* **105**, 21–31. (doi:10.1016/S0031-9201(97)00077-0.)

Fiquet, G., Dewaele, A., Andrault, D., Kunz, M. & le Bihan, T. 2000 Thermoelastic properties and crystal structure of $MgSiO_3$ perovskite at lower mantle pressure and temperature conditions. *Geophys. Res. Lett.* **27**, 21–24. (doi:10.1029/1999GL008397.)

Fiquet, G., Badro, J., Guyot, F., Requardt, H. & Krisch, M. 2001 Sound velocities in iron to 110 GPa. *Science* **291**, 468–471. (doi:10.1126/science.291.5503.468.)

Fiquet, G. *et al.* 2004 Application in inelastic X-ray scattering to the measurements of acoustic wave velocities in geophysical materials at very high pressure. *Phys. Earth Planet. In.* **143–144**, 5–18. (doi:10.1016/j.pepi.2003.10.005.)

Flesch, L. M., Li, B. & Liebermann, R. C. 1998 Sound velocities of polycrystalline $MgSiO_3$-orthopyroxene to 10 GPa at room temperature. *Am. Mineral.* **83**, 444–450.

Forte, A. M. & Mitrovica, J. X. 2001 Deep-mantle high-viscosity flow and thermochemical structure inferred from seismic and geodynamic data. *Nature* **410**, 1049–1056. (doi:10.1038/35074000.)

Francis, D. 2003 Cratonic mantle roots, remnants of a more chondritic Archean mantle? *Lithos* **71**, 135–152. (doi:10.1016/S0024-4937(03)00110-5.)

Garnero, E. J., Maupin, V., Lay, T. & Fouch, M. J. 2004 Variable azimuthal anisotropy in Earth's lowermost mantle. *Science* **306**, 259–261. (doi:10.1126/science.1103411.)

Gwanmesia, G. D., Chen, G. & Liebermann, R. C. 1998 Sound velocities in $MgSiO_3$-garnet to 8 GPa. *Geophys. Res. Lett.* **25**, 4553–4556. (doi:10.1029/1998GL900189.)

Hall, S. A., Kendall, J. M. & van der Baan, M. 2004 Some comments on the effects of lower-mantle anisotropy on SKS and SKKS phases. *Phys. Earth Planet. In.* **146**, 469–481. (doi:10.1016/j.pepi.2004.05.002.)

Hama, J. & Suito, K. 2001 Thermoelastic models of minerals and the composition of the Earth's lower mantle. *Phys. Earth Planet. In.* **125**, 147–166. (doi:10.1016/S0031-9201(01)00248-5.)

Helffrich, G. R. 2002 Chemical and seismological constraints on mantle heterogeneity. *Phil. Trans. R. Soc. A* **360**, 2493–2505. (doi:10.1098/rsta.2002.1085.)

Helffrich, G. R. & Wood, B. J. 2001 The Earth's mantle. *Nature* **412**, 501–507. (doi:10.1038/35087500.)

Horiuchi, H., Ito, E. & Weidner, D. J. 1987 Perovskite-type $MgSiO_3$: single-crystal X-ray diffraction study. *Am. Mineral.* **72**, 357–360.

Iitaka, T., Hirose, K., Kawamura, K. & Murakami, M. 2004 The elasticity of the $MgSiO_3$ post-perovskite phase in the Earth's lowermost mantle. *Nature* **430**, 442–445. (doi:10.1038/nature02702.)

Inoue, H., Fukao, Y., Tanabe, K. & Ogata, Y. 1990 Whole mantle P-wave travel time tomography. *Phys. Earth Planet. In.* **90**, 294–328. (doi:10.1016/0031-9201(90)90236-Q.)

Irifune, T. 1994 Absence of an aluminous phase in the upper part of the Earth's lower mantle. *Nature* **370**, 131–133. (doi:10.1038/370131a0.)

Irifune, T., Koizumi, T. & Ando, J. I. 1996 An experimental study of the garnet–perovskite transformation in the system $MgSiO_3$–$Mg_3Al_2Si_3O_{12}$. *Phys. Earth Planet. In.* **96**, 147–157. (doi:10.1016/0031-9201(96)03147-0.)

Isaak, D. G., Anderson, O. L. & Goto, T. 1989 Measured elastic moduli of single crystal MgO up to 1800 K. *Phys. Chem. Miner.* **16**, 704–713. (doi:10.1007/BF00223321.)

Isaak, D. G., Anderson, O. L. & Cohen, R. E. 1992 The relationship between shear and compressional velocities at high pressures: reconciliation of seismic tomography and mineral physics. *Geophys. Res. Lett.* **19**, 741–744.

Ishii, M. & Tromp, J. 1999 Normal-mode and free-air gravity constraints on lateral variations in velocity and density of Earth's mantle. *Science* **285**, 1231–1236. (doi:10.1126/science.285.5431.1231.)

Ito, E. & Takahashi, E. 1987 Ultrahigh-pressure phase transformations and the constitution of the deep mantle. In *High-pressure research in mineral physics*, vol. 2 (ed. M. H. Manghnani & Y. Syono). Geophysical monographs 39. Mineral Physics, pp. 221–229. Washington, DC: American Geophysical Union.

Ito, E., Takahashi, E. & Matsui, Y. 1984 The mineralogy and chemistry of the lower mantle—an implication of the ultrahigh-pressure phase relations in the system MgO–FeO–SiO_2. *Earth Planet. Sci. Lett.* **67**, 238–248. (doi:10.1016/0012-821X(84)90119-5.)

Jackson, I. 1998 Elasticity, composition and temperature of the Earth's lower mantle: a reappraisal. *Geophys. J. Int.* **134**, 291–311. (doi:10.1046/j.1365-246x.1998.00560.x.)

Jackson, I. & Rigden, S. M. 1998 Composition and temperature of the Earth's mantle: seismological models interpreted through experimental studies of mantle materials. In *The Earth's mantle: composition, structure and evolution* (ed. I. Jackson), pp. 405–460. New York: Cambridge University Press.

Jackson, I., Khanna, S. K., Revcolevschi, A. & Berthon, J. 1990 Elasticity, shear-mode softening and high pressure polymorphism of wüstite ($Fe_{1-x}O$). *J. Geophys. Res.* **95**, 21 671–21 685.

Jackson, J. M., Zhang, J. Z. & Bass, J. D. 2004 Sound velocities and elasticity of aluminous $MgSiO_3$ perovskite: implications of aluminium heterogeneity in Earth's lower mantle. *Geophys. Res. Lett.* **31**, L10 614. MAY 27. (doi:10.1029/2004GL019918.)

Jackson, I., Webb, S., Weston, L. & Boness, D. 2005 Frequency dependence of elastic wave speeds at high temperature: a direct experimental demonstration. *Phys. Earth Planet. In.* **148**, 85–96. (doi:10.1016/j.pepi.2004.08.004.)

Jacobsen, S. D., Spetzler, H. A., Reichmann, H. J., Smyth, J. R., Mackwell, S. J., Angel, R. J. & Bassett, W. A. 2002 Gigahertz ultrasonic interferometry at high P and T: new tools for obtaining a thermodynamic equation of state. *J. Phys.: Condens. Mater.* **14**, 11 525–11 530. (doi:10.1088/0953-8984/14/44/510.) (SO953-8984(02)39391-3)

Jacobsen, S. D., Spetzler, H., Reichmann, H. J. & Smyth, J. R. 2004 Shear waves in the diamond-anvil cell reveal pressure-induced instability in (Mg,Fe)O. *Proc. Natl Acad. Sci. USA* **101**, 5867–5871. (doi:10.1073/pnas.0401564101.)

Javoy, M. 1999 Chemical Earth models. *C. R. Acad. Sci. Paris* **329**, 537–555.

Jeanloz, R. & Knittle, E. 1989 Density and composition of the lower mantle. *Phil. Trans. R. Soc. A* **328**, 377–389.

Karato, S. 1993 Importance of anelasticity in the interpretation of seismic tomography. *Geophys. Res. Lett.* **20**, 1623–1626.

Karato, S. & Karki, B. B. 2001 Origin of lateral variation in seismic wave velocities. *J. Geophys. Res.* **106**, 21 771–21 783. (doi:10.1029/2001JB000214.)

Karki, B. B. & Crain, J. 1998 First-principles determination of elastic properties of $CaSiO_3$ perovskite at lower mantle pressures. *Geophys. Res. Lett.* **25**, 2741–2744. (doi:10.1029/98GL51952.)

Karki, B. B. & Stixrude, L. 1999 Seismic velocities of major silicate and oxide-phases of the lower mantle. *J. Geophys. Res.* **104**, 13 025–13 033. (doi:10.1029/1999JB900069.)

Karki, B. B., Stixrude, L., Clark, S. J., Warren, M. C., Ackland, G. J. & Crain, J. 1997*a* Structure and elasticity of MgO at high pressure. *Am. Mineral.* **82**, 51–60.

Karki, B. B., Stixrude, L., Clark, S. J., Warren, M. C., Ackland, G. J. & Crain, J. 1997*b* Elastic properties of orthorhombic $MgSiO_3$ perovskite at lower mantle pressures. *Am. Mineral.* **82**, 635–638.

Karki, B. B., Wentzcovitch, R. M., de Gironcoli, S. & Baroni, S. 1999 First-principles determination of elastic anisotropy and wave velocities of MgO at lower mantle conditions. *Science* **286**, 1705–1707. (doi:10.1126/science.286.5445.1705.)

Katsura, T. & Ito, E. 1996 Determination of Fe–Mg partitioning between perovskite and magnesiowüstite. *Geophys. Res. Lett.* **23**, 2005–2008. (doi:10.1029/96GL02086.)

Kellogg, L. H., Hager, B. H. & van der Hilst, R. D. 1999 Compositional stratification in the deep mantle. *Science* **283**, 1881–1884. (doi:10.1126/science.283.5409.1881.)

Kennett, B. L. N., Engdahl, E. R. & Buland, R. 1995 Constraints on seismic velocities in the Earth from traveltimes. *Geophys. J. Int.* **122**, 108–124.

Kennett, B. L. N., Widiyantoro, S. & van der Hilst, R. D. 1998 Joint seismic tomography for bulk sound and shear wave speed in the Earth's mantle. *J. Geophys. Res.* **103**, 12 469–12 493. (doi:10.1029/98JB00150.)

Kesson, S. E., Fitz Gerald, J. D., Shelley, J. M. G. & Withers, R. L. 1995 Phase-relations, structure and crystal-chemistry of some aluminous silicate perovskites. *Earth Planet. Sci. Lett.* **134**, 187–201. (doi:10.1016/0012-821X(95)00112-P.)

Kesson, S., Ringwood, A. E., Hibberson, W., Fitz Gerald, J. & Ware, N. 1997 Reaction between magnesiowüstite of lower mantle composition and core-forming Fe–Ni alloy at 1–40 GPa. *Am. Mineral.* **82**, 526–533.

Kiefer, B., Stixrude, L. & Wentzcovitch, R. M. 2002 Elasticity of (Mg,Fe)SiO_3-perovskite at high pressures. *Geophys. Res. Lett.* **29**, 34. (doi:10.1029/2002GL014683.) 101029/2002GL014683.

Kohn, W. & Sham, L. J. 1965 Self-consistent equations including exchange and correlation effects. *Phys. Rev.* **140**, A1133–A1138. (doi:10.1103/PhysRev.140.A1133.)

Kondo, T., Ohtani, E., Hirao, N., Yagi, T. & Kikegawa, T. 2004 Phase transitions of (Mg,Fe)O at megabar pressures. *Phys. Earth Planet. In.* **143–144**, 201–213. (doi:10.1016/j.pepi.2003.10.008.)

Lay, T., Williams, Q. & Garnero, E. J. 1998 The core–mantle boundary layer and deep Earth dynamics. *Nature* **392**, 461–468. (doi:10.1038/33083.)

Lee, K. K. M., O'Neill, B., Panero, W. R., Shin, S. H., Benedetti, L. R. & Jeanloz, R. 2004 Equations of state of high-pressure phases of a natural peridotite and implications for the Earth's lower mantle. *Earth Planet. Sci. Lett.* **221**, 381–393. (doi:10.1016/j.epsl.2004.04.033.)

Li, J. & Agee, C. B. 1996 Geochemistry of mantle–core differentiation at high pressure. *Nature* **381**, 686–689. (doi:10.1038/381686a0.)

Li, B. & Liebermann, R. C. 2000 Sound velocities of wadsleyite beta-$(Mg_{0.88}Fe_{0.12})_2SiO_4$ to 10 GPa. *Am. Mineral.* **85**, 292–295.

Li, B., Chen, G., Gwanmesia, G. D. & Liebermann, R. C. 1998 Sound velocity measurements at mantle transition zone conditions of pressure and temperature using ultrasonic interferometry in a multi-anvil apparatus. In *Properties of Earth and planetary materials at high pressure and temperature* (ed. M. H. Manghnani & T. Yagl). Geophysical monograph 101, pp. 41–61. Washington, DC: American Geophysical Union.

Li, B., Liebermann, R. C. & Wiedner, D. J. 2001 P–V–V_P–V_S–T measurements on wadsleyite to 7 GPa and 873 K: implications for the 410 km seismic discontinuity. *J. Geophys. Res.* **106**, 30 575–30 591.

Li, B., Kung, J. & Liebermann, R. C. 2004*a* Modern techniques in measuring elasticity of Earth materials at high pressure and high temperature using ultrasonic interferometry in conjunction with synchrotron X-radiation in multi-anvil apparatus. *Phys. Earth Planet. In.* **143–144**, 559–574. (doi:10.1016/j.pepi.2003.09.020.)

Li, J. *et al.* 2004*b* Electronic spin state of iron in lower mantle perovskite. *Proc. Natl. Acad. Sci. USA* **101**, 14 027–14 030. (doi:10.1073/pnas.0405804101.)

Lin, J. F., Heinz, D. L., Mao, H. K., Hemley, R. J., Devine, J. M., Li, J. & Shen, G. 2003 Stability of magnesiowüstite in Earth's lower mantle. *Proc. Natl. Acad. Sci. USA* **100**, 4405–4408. (doi:10.1073/pnas.252782399.)

Liu, L. G. 1979 Phase transformations and constitution of the deep mantle. In *The earth: its origin, structure and evolution* (ed. M. W. McEihinney), pp. 177–202. London: Academic Press.

Liu, L. & Ringwood, A. E. 1975 Synthesis of a perovskite-type polymorph of $CaSiO_3$. *Earth Planet. Sci. Lett.* **14**, 209–211. (doi:10.1016/0012-821X(75)90229-0.)

Liu, L., Mernagh, T. P. & Irifune, T. 1995 Raman spectra of $MgSiO_3 \cdot 10\%$ Al_2O_3-perovskite at various pressures and temperatures. *Phys. Chem. Miner.* **22**, 511–516.

Lundqvist, S. & March, N. H. 1983 *Theory of the inhomogeneous electron gas.* New York: Plenum Press.

Mao, H. K. & Bell, P. M. 1979 Equation of state of MgO and eta-Fe under static pressure conditions. *J. Geophys. Res.* **84**, 4533–4536.

Mao, H. K., Chen, L. C., Hemley, R. J., Jephcoat, A. P., Wu, Y. & Bassett, W. A. 1989 Stability and equation of state of $CaSiO_3$ perovskite to 134 GPa. *J. Geophys. Res.* **94**, 17 889–17 894.

Mao, H. K., Hemley, R. J., Fei, Y., Shu, J. F., Chen, L. C., Jephcoat, A. P., Wu, Y. & Bassett, W. A. 1991 Effect of pressure, temperature and composition of lattice parameters and density of $(Fe,Mg)SiO_3$ perovskite to 30 GPa. *J. Geophys. Res.* **96**, 8069–8079.

Mao, H. K., Shu, J. F., Fei, Y. W., Hu, J. Z. & Hemley, R. J. 1996 The wüstite enigma. *Phys. Earth Planet. In.* **96**, 135–145. (doi:10.1016/0031-9201(96)03146-9.)

Mao, H. K., Shen, G. Y. & Hemley, R. J. 1997 Multivariable dependence of Fe–Mg partitioning in the lower mantle. *Science* **278**, 2098–2100. (doi:10.1126/science.278.5346.2098.)

Mao, H. K., Shu, J., Shen, G., Hemley, R. J., Li, B. & Singh, A. K. 1998 Elasticity and rheology of iron above 220 GPa and the nature of the Earth's inner core. *Nature* **396**, 741–743. (doi:10.1038/25506.). [Erratum in *Nature* **399**, 280.]

Marton, F. C. & Cohen, R. E. 2002 Constraints on lower mantle composition from molecular dynamics simulations of $MgSiO_3$ perovskite. *Phys. Earth. Planet. In.* **134**, 239–252.

Marx, D. & Hutter, J. 2000 *Ab initio* molecular dynamics: theory and implementation. In *Modern methods and algorithms of quantum chemistry* (ed. J. Grotendorst) NIC Series, vol. 1, pp. 301–449. Jülich: John von Newmann Institute for computing.

Masters, G., Laske, G., Bolton, H. & Dziewonski, A. 2000 The relative behaviour of shear velocity, bulk sound speed and compressional velocity in the mantle: implications for chemical and thermal structure. In *Earth's deep interior: mineral physics and tomography from the atomic to the global scale* (ed. S. Karato, A. M. Forte, R. C. Liebermann, G. Masters & L. Stixrude). Geophysical monograph 117, pp. 63–87. Washington, DC: American Geophysical Union.

McCammon, C. 1997 Perovskite as a possible sink for ferric iron in the lower mantle. *Nature* **387**, 694–696. (doi:10.1038/42685.)

Murakami, M., Hirose, K., Kawamura, K., Sata, N. & Ohishi, Y. 2004 Post-perovskite phase transition in $MgSiO_3$. *Science* **304**, 855–858. (doi:10.1126/science.1095932.)

Nye, J. F. 1985 *Physical properties of crystals: their representation by tensors and matrices.* Oxford: Oxford University Press.

Oganov, A. R. & Brodholt, J. P. 2000 High-pressure phases in the Al_2SiO_5 system and the problem of aluminous phase in the Earth's lower mantle: ab inito calculations. *Phys. Chem. Miner.* **27**, 430–439. (doi:10.1007/s002699900081.)

Oganov, A. R. & Dorogokupets, P. I. 2003 All-electron and pseudopotential study of MgO: equation of state, anharmonicity, and stability. *Phys. Rev. B* **67**, 0163-1829/2003/67(22) /224110(11). (doi:10.1103/PhysRevB.67.224110.)

Oganov, A. R. & Ono, S. 2004 Theoretical and experimental evidence for a post-perovskite phase of $MgSiO_3$ in Earth's D″ layer. *Nature* **430**, 445–448. (doi:10.1038/nature02701.)

Oganov, A. R., Brodholt, J. P. & Price, G. D. 2001*a* *Ab initio* elasticity and thermal equation of state of $MgSiO_3$ perovskite. *Earth Planet. Sci. Lett.* **184**, 555–560. (doi:10.1016/S0012-821X(00)00363-0.)

Oganov, A. R., Brodholt, J. P. & Price, G. D. 2001*b* The elastic constants of $MgSiO_3$ perovskite at pressures and temperatures of the Earth's mantle. *Nature* **411**, 934–937. (doi:10.1038/35082048.)

Oguri, K., Funamori, N., Sakai, F., Kondo, T., Uchida, T. & Yagi, T. 1997 High-pressure and high-temperature phase relations in diopside $CaMgSi_2O_6$. *Phys. Earth Planet. In.* **104**, 363–370. (doi:10.1016/S0031-9201(97)00029-0.)

Oldham, D. & Davies, J. H. 2004 Numerical investigation of layered convection in a three-dimensional shell with application to planetary mantles. *Geochem. Geophys. Geosyst.* **5**, Q12C04. DEC 31. (doi:10.1029/2003GC000603.)

O'Neill, H. St. C. 1991 The origin of the Moon and the early history of the Earth—a chemical model. Part 2: the Earth. *Geochim. Cosmochim. Acta* **55**, 1159–1172. (doi:10.1016/0016-7037(91)90169-6.)

O'Neill, B. & Jeanloz, R. 1994 $MgSiO_3$–$FeSiO_3$–Al_2O_3 in the Earth's lower mantle: perovskite and garnet at 1200 km depth. *J. Geophys. Res.* **99**, 19 901–19 915. (doi:10.1029/94JB01752.)

Perdew, J. P., Burke, K. & Ernzerhof, M. 1996 Generalized gradient approximation made simple. *Phys. Rev. Lett.* **77**, 3865–3868. (doi:10.1103/PhysRevLett.77.3865.)

Pickett, W. E. 1989 Pseudopotentials in condensed matter systems. *Comp. Phys. Rep.* **9**, 114–197. (doi:10.1016/0167-7977(89)90002-6.)

Poirier, J. P. 1995 All the latest on… the centre of the Earth. *Recherche* **282**, 108–111.

Pollard, H. F. 1977 *Sound waves in solids.* Pion applied series 9. London: Pion Limited.

Price, G. D. & Vočădlo, L. 1996 Computational mineralogy. *Comptes Rendus de l'academie des sciences serie II Fascicle A—Sciences de la terre et des planetes* **313**, 357–371.

Reichmann, H. J. & Jacobsen, S. D. 2004 High-pressure elasticity of a natural magnetite crystal. *Am. Mineral.* **89**, 1061–1066.

Reichmann, H. J., Angel, R. J., Spetzler, H. & Bassett, W. A. 1998 Ultrasonic interferometry and X-ray measurements on MgO in a new diamond anvil cell. *Am. Mineral.* **83**, 1357–1360.

Reichmann, H. J., Jacobsen, S. D., Mackwell, S. J. & McCammon, C. A. 2000 Sound velocities and elastic constants for magnesiowüstite using gigahertz interferometry. *Geophys. Res. Lett.* **27**, 799–802. (doi:10.1029/1999GL008411.)

Ringwood, A. E. 1975 *Composition and petrology of the Earth's mantle.* McGraw-Hill International series in the Earth and planetary sciences. New York: McGraw-Hill.

Ringwood, A. E. 1979 Composition and origin of the earth. In *The earth: its origin, structure and evolution* (ed. M. W. McEihinney), pp. 1–59. London: Academic Press.

Robertson, G. S. & Woodhouse, J. H. 1996 Constraints on lower mantle physical properties from seismology and mineral physics. *Earth Planet. Sci. Lett.* **143**, 197–205. (doi:10.1016/0012-821X(96)00134-3.)

Ross, N. L. & Hazen, R. M. 1990 High pressure crystal chemistry of $MgSiO_3$ perovskite. *Phys. Chem. Miner.* **17**, 228–237. (doi:10.1007/BF00201454.)

Shen, A. H., Reichmann, H. J., Chen, G., Angel, R. J., Bassett, W. A. & Spetzler, H. 1998 GHz ultrasonic interferometry in a diamond anvil cell: P-wave velocities in periclase to 4.4 GPa and 207 C. In *Properties of Earth and planetary materials at high pressure and temperature* (ed. M. H. Manghnani & T. Yagi). Geophysical monograph 101, pp. 71–77. Washington DC: American Geophysical Union.

Sherman, D. M. 1993 Equation of state, elastic properties and stability of $CaSiO_3$ perovskite: first principles (Periodic Hartree Fock) result. *J. Geophys. Res.* **98**, 19 795–19 805.

Shieh, S. R., Duffy, T. S. & Shen, G. 2004 Elasticity and strength of calcium silicate perovskite at lower mantle pressures. *Phys. Earth Planet. In.* **143-144**, 95–105.

Shim, S. H., Duffy, T. S. & Shen, G. 2000*a* The stability and *P*–*V*–*T* equation of state of $CaSiO_3$ perovskite in the Earth's lower mantle. *J. Geophys. Res.* **105**, 25 955–25 968. (doi:10.1029/2000JB900183.)

Shim, S. H., Duffy, T. S. & Shen, G. 2000*b* The equation of state of $CaSiO_3$ perovskite to 108 GPa and 300 K. *Phys. Earth Planet. In.* **120**, 327–338. (doi:10.1016/S0031-9201(00)00154-0.)

Shito, A. & Shibutani, T. 2001 Upper mantle transition zone structure beneath the Philippine sea region. *Geophys. Res. Lett.* **28**, 871–874. (doi:10.1029/2000GL012235.)

Sinelnikov, Y. D., Chen, G., Neuville, D. R., Vaughan, M. T. & Liebermann, R. C. 1998 Ultrasonic shear wave velocities of $MgSiO_3$ perovskite at 8 GPa and 800 K and lower mantle composition. *Science* **281**, 677–678. (doi:10.1126/science.281.5377.677.)

Sinogeikin, S. V. & Bass, J. D. 1999 Single-crystal elasticity of MgO at high pressure. *Condens. Matter Mater. Sci.* **59**, 0163-1829/99/59(22)/14141(4).

Sinogeikin, S. V. & Bass, J. D. 2000 Single crystal elasticity of pyrope and MgO to 20 GPa by Brillouin scattering in the diamond cell. *Phys. Earth Planet. In.* **120**, 43–62.

Sinogeikin, S. V., Lakshtanov, D. L., Nicholas, J. D. & Bass, J. D. 2004 Sound velocity measurements on laser-heated MgO and Al_2O_3. *Phys. Earth Planet. In.* **143–144**, 575–586. (doi:10.1016/j.pepi.2003.09.017.)

Stixrude, L. 2000 Elasticity of mantle phases at high pressure and temperature. In *Earth's deep interior: mineral physics and tomography from the atomic to the global scale* (ed. S. Karato, A. M. Forte, R. C. Liebermann, G. Masters & L. Stixrude). Geophysical monograph 117, pp. 201–213. Washington, DC: American Geophysical Union.

Stixrude, L., Hemley, R. J., Fei, Y. & Mao, H. K. 1992 Thermoelasticity of silicates perovskite and magnesiowüstite and stratification of the Earth's mantle. *Science* **257**, 1099–1101.

Stølen, S. & Grønvold, F. 1996 Calculation of the phase boundaries of wüstite at high pressure. *J. Geophys. Res.* **101**, 11 531–11 540.

Tamai, H. & Yagi, T. 1989 High-pressure and high-temperature phase relations in $CaSiO_3$ and $CaMgSi_3O_4$ and elasticity of perovskite type $CaSiO_3$. *Phys. Earth Planet. In.* **54**, 370–377. (doi:10.1016/0031-9201(89)90254-9.)

Tarrida, M. & Richet, P. 1989 Equation of state of $CaSiO_3$ perovskite to 96 GPa. *Geophys. Res. Lett.* **16**, 1351–1354.

Thomas, C., Kendall, J. M. & Lowman, J. 2004 Lower-mantle seismic discontinuities and the thermal morphology of subducted slabs. *Earth Planet. Sci. Lett.* **225**, 105–113. (doi:10.1016/j.epsl.2004.05.038.)

Trampert, J., Deschamps, F., Resovsky, J. & Yuen, D. 2004 Probabilistic tomography maps chemical heterogeneities throughout the lower mantle. *Science* **306**, 853–856. (doi:10.1126/science.1101996.)

van der Hilst, R. D. & Karason, H. 1999 Compositional heterogeneity in the bottom 1000 kilometers of Earth's mantle: toward a hybrid convection model. *Science* **283**, 1885–1888. (doi:10.1126/science.283.5409.1885.)

Vidale, J. E., Schubert, G. & Earle, P. S. 2001 Unsuccessful initial search for a midmantle chemical boundary with seismic arrays. *Geophys. Res. Lett.* **28**, 859–862. (doi:10.1029/2000GL012428.)

Wallace, D. C. 1970 Thermoelastic theory of stressed crystals and higher-order elastic constants. In *Solid state physics advances in research and applications* (ed. H. Ehrenreich, F. Seitz & D. Turnbull), pp. 301–404. London: Academic Press.

Walter, M. J. & Trønnes, R. G. 2004 Early Earth differentiation. *Earth Planet. Sci. Lett.* **225**, 253–269. (doi:10.1016/j.epsl.2004.07.008.)

Walter, M. J., Kubo, A., Yoshino, T., Brodholt, J., Koga, K. T. & Ohishi, Y. 2004 Phase relations and equations-of-state of aluminous Mg-silicate perovskite and implications for Earth's lower mantle. *Earth Planet. Sci. Lett.* **222**, 501–516. (doi:10.1016/j.epsl.2004.03.014.)

Wang, Y. & Weidner, D. J. 1994 Thermoelasticity of $CaSiO_3$ perovskite and implications for the lower mantle. *Geophys. Res. Lett.* **21**, 895–898. (doi:10.1029/94GL00976.)

Wang, Y. & Weidner, D. J. 1996 $(\partial G/\partial T)_\mathrm{P}$ of the lower mantle. *Pure Appl. Geophys.* **146**, 533–549. (doi:10.1007/BF00874732.)

Wang, Y., Weidner, D. J. & Guyot, F. 1996 Thermal equation of state of $\mathrm{CaSiO_3}$ perovskite. *J. Geophys. Res.* **101**, 661–672. (doi:10.1029/95JB03254.)

Warren, M. C., Ackland, G. J., Karki, B. B. & Clark, S. J. 1998 Phase transitions in silicate perovskites from first principles. *Min. Mag.* **62**, 585–598.

Weidner, D. J. & Zhao, Y. 1992 The structural distortion of perovskite and its implication to the lower mantle. In *High pressure research: applications to Earth and planetary sciences* (ed. Y. Syono & M. H. Manghnani), pp. 191–196. Washington, DC: American Geophysical Union.

Wentzcovitch, R. M., Karki, B. B., Karato, S. & Da Silva, C. R. S. 1998 High pressure elastic anisotropy of $\mathrm{MgSiO_3}$ perovskite and geophysical implications. *Earth Planet. Sci. Lett.* **164**, 371–378. (doi:10.1016/S0012-821X(98)00230-1.)

Widiyantoro, S., Kennett, B. L. N. & van der Hilst, R. D. 1999 Seismic tomography with P and S data reveals lateral variations in the rigidity of deep slabs. *Earth Planet. Sci. Lett.* **173**, 91–100. (doi:10.1016/S0012-821X(99)00216-2.)

Wood, B. J. 1993 Carbon in the core. *Earth Planet. Sci. Lett.* **117**, 593–607. (doi:10.1016/0012-821X(93)90105-I.)

Wood, B. J. & Rubie, D. C. 1996 The effect of alumina on phase transformations at the 660 kilometer discontinuity from Fe–Mg partitioning experiments. *Science* **273**, 1522–1524.

Woodhouse, J. H. & Dziewonski, A. M. 1989 Seismic modelling of the Earth's large-scale three-dimensional structure. *Phil. Trans. R. Soc. A* **328**, 291–308.

Yagi, T., Okabe, K., Nishiyama, N., Kubo, A. & Kikegawa, T. 2004 Complicated effects of aluminium on the compressibility of silicate perovskite. *Phys. Earth Planet. In.* **143–144**, 81–91. (doi:10.1016/j.pepi.2003.07.020.)

Yeganeh-Haeri, A. 1994 Synthesis and re-investigation of the elastic properties of single-crystal magnesium silicate perovskite. *Phys. Earth Planet. In.* **87**, 111–121. (doi:10.1016/0031-9201(94)90025-6.)

Yeganeh-Haeri, A. & Weidner, D. J. 1989 Elasticity of $\mathrm{MgSiO_3}$ in the perovskite structure. *Science* **243**, 787–789.

Yoneda, A. 1990 Pressure derivatives of elastic constants of single crystal MgO and $\mathrm{MgAl_2O_4}$. *J. Phys. Earth.* **38**, 19–55.

Zha, C. S., Mao, H. K. & Hemley, R. J. 2000 Elasticity of MgO as primary pressure scale to 55 GPa. *Proc. Natl Acad. Sci. USA* **97**, 13 494–13 499. (doi:10.1073/pnas.240466697.)

Zhang, J. & Kostak Jr, P. 2002 Thermal equation of state of magnesiowüstite $\mathrm{(Mg_{0.6}Fe_{0.4})O}$. *Phys. Earth Planet. In.* **129**, 301–311. (doi:10.1016/S0031-9201(01)00296-5.)

Zhang, J. & Weidner, D. J. 1999 *Thermal equation of state of aluminium-enriched silicate perovskite. Science* **284**, 782–784.

Zhao, Y. & Anderson, D. L. 1994 Mineral physics constraints on the chemical composition of the Earth's lower mantle. *Phys. Earth Planet. In.* **85**, 273–292. (doi:10.1016/0031-9201(94)90118-X.)

Zhao, Y., Weidner, D. J. & SAM-85 team 1994 Perovskite at high P–T conditions: an *in situ* synchrotron x-ray diffraction study of $\mathrm{NaMgF_3}$ perovskite *J. Geophys. Res.* **99** 2871–2885. (doi:10.1029/93JB02757.)